The Propagation of Surface Waves in Flow Down an Oscillating Inclined Plane

Steven J. Weinstein
Emulsion Coating Technologies, Eastman Kodak Company, Rochester, NY 14652

Jean-Marie Baumlin and Jeanne Servant
Centre de Recherches et de Technologie, Kodak-Pathe, Chalon-sur-Saone 71102, France

The propagation of surface waves is investigated theoretically and experimentally for the case of a single layer of viscous liquid flowing down an inclined plane, where the plane is oscillating in the flow direction. This work focuses on the linearized wavemaker problem, where the oscillations create waves which are small perturbations from the undisturbed flow. Downstream from the entrance region to the incline where the fluid is introduced, the undisturbed interface is parallel to the incline surface, and theory predicts that oscillations do not interact with waves that travel along the free surface. These waves grow as if there were no oscillation at all, and their propagation is governed by a dispersion relation between frequency, wavelength, and wave growth for single layer flow down a nonoscillating inclined plane. The entrance region to the incline is therefore responsible for exciting the various wave frequencies which are observed down the incline, as well as the initial amplitude of these waves. Experiments performed verify that waves propagate as predicted. Theory indicates that these conclusions are valid when the oscillations are perpendicular to the incline, as well as for the case of multiple stacked layers.

Introduction

There are many industrial applications where solids are coated with thin liquid films, from the enhancement of heat and mass transfer on solids to the production of various thin-film coatings. In slide coating operations, for example, the flow of a fluid down an inclined plane is a fundamental step in the production of multiple-layer products. The inclined plane provides a means by which fluid layers can be stacked on top of one another; at the end of the incline, a moving substrate is coated with these fluid layers. The ideal flow has all the fluid layers parallel to the solid inclined surface. However, in practice, there are a variety of disturbances which can distort the fluid flow away from this parallel structure in the form of waves. These waves not only translate down the incline in the direction of the bulk fluid flow, but they also grow or decay depending on the specific flow conditions and fluid properties of the system in question. Waves can give rise to thickness variations in the fluid layers, which can subsequently translate into the coated substrate; this is clearly undesirable when attempting to make uniform coatings. It is thus necessary to understand the nature of wave formation and propagation in these flows.

The first experimental and theoretical studies of film flows down inclined surfaces focused on the neutral stability of single-layer Newtonian fluids, that is, whether an infinitesimal flow disturbance would grow or decay (Benjamin, 1957; Binnie, 1957; Yih, 1963; for an extensive review of the initial work in this area, see Krantz and Goren, 1971), as well as the critical wavelength and wave speed of the fastest growing wave; primarily, room noise was used to induce these waves to form in experiments. These studies showed that neutral stability of single layers of thickness, d, could be deduced by investigating the limit of small wavenumber, α, where $\alpha = 2\pi d/\lambda$, and λ is the wavelength. Furthermore, the fastest growing waves typically occurred at values of $\alpha < 1$ (long wavelengths). In this range of wavenumber, the spatial damping (as well as wavelengths and wave speeds) of the waves away from neutrally stable conditions was investigated both experimentally and theoretically by Krantz and Goren (1971). Experimentally, a

Correspondence concerning this article should be addressed to S. J. Weinstein.

wire stretched across the width of the incline was used as a controlled input to excite waves, and a light-extinction technique was used to measure the wave-propagation characteristics. Theoretical wave damping and wave speed predictions were in qualitative agreement with experimental results, the most notable discrepancies being in wave speed. Using a more accurate approximate theoretical technique, Krantz and Owens (1973) obtained quantitative agreement with experiment for the wave damping, although the wave speed calculations still underpredicted the experimental results. Baumlin and Pasquet (1988) experimentally investigated the spatial damping of surface waves for $\alpha > 1$, employing flow rate pulsations to excite waves; these experiments agreed quite well with their theoretical predictions.

The flow of multiple-layer Newtonian fluids down an incline has also been considered theoretically. Kao (1965a,b, 1968) investigated the effect of viscosity and density stratification in two-layer systems on the stability of the flow, restricting attention to the long wavelength limit ($\alpha \to 0$). Akhtaruzzaman et al. (1978) investigated the $\alpha \to 0$ motion of a three-layer system, the stability of which was subsequently determined by Wang et al. (1978). For zero Reynolds number, Loewenherz and Lawrence (1989) demonstrated that the largest growth of waves in multiple-layer systems can occur at finite wavelengths, where these wavelengths are not accessible in the $\alpha \to 0$ limit. This behavior has also been seen by Weinstein (1990) for finite Reynolds numbers; thus, long wavelength analyses often do not allow the study of the fastest growing waves in multiple-layer flow down an inclined plane.

Whether or not single- or multiple-layer flows are considered, the theoretical analyses in the above literature have a similar structure; an eigenvalue problem is solved to find the dispersion relation among the wavelength, frequency, and wave growth. The allowable wave modes from this eigenvalue problem are valid presuming that the waves can be viewed as small perturbations away from a uniform, rectilinear flow. Thus, they are not valid in the region to the incline where the flow is first introduced (henceforth called the entrance region), since the undisturbed flow field is adjusting to changes in boundary conditions at the entrance to the incline and the flow is not rectilinear there (Figure 1). The previous literature can be viewed as giving the wave modes valid away from the entrance region where the flow is rectilinear (this region will be called the uniform film region). If disturbances which cause the waves to form are found in the uniform film region, then certain wave modes from the previous literature will be excited directly. On the other hand, if disturbances impinge on the flow in the entrance region to the incline, the physics of this region will determine the amplitudes and frequencies of the waves which are excited and observed down the incline in the uniform film region.

A question arises, however, as to how the propagation characteristics of the waves in the uniform film region are altered when the solid incline surface (hereafter called the wall) is oscillating with a given frequency. Baikov et al. (1983) investigated how the long wavelength stability of a single Newtonian layer is affected by a wall which oscillates in the direction of flow. When the oscillation is on the same order as the average velocity of the fluid flow, there is a significant effect on the neutral stability of the flow. However, when the magnitude of the velocity oscillation is small relative to the average velocity

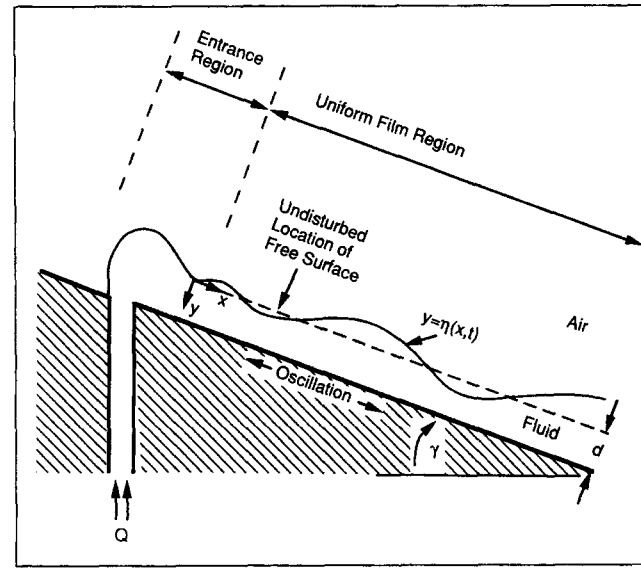

Figure 1. Typical geometry of the entrance region and uniform film region

of the fluid, there is little effect on the neutral stability; in fact, this effect is of $O(\epsilon^2)$, where ϵ is the magnitude of the oscillation. Thus, in the linear approximation, $O(\epsilon)$, the oscillations have no effect on the long wavelength stability of the flow. Bauer and von Kerczek (1991) obtained the same analytic long wavelength stability results as Baikov et al. (1983), but employed numerical techniques to predict the growth of waves at finite wavelengths. Bauer and von Kerczek demonstrate that the inclined plane flow can be stabilized by sufficiently large amplitude wall oscillations. However, because of the numerical approach necessary to investigate these large amplitudes, an explicit solution is not given which shows how linear disturbances, that is, small amplitude wall oscillations, affect waves at *finite* wavelengths. Furthermore, they formulate the problem for temporally growing waves, while in many coating applications, waves grow spatially (Weinstein, 1990).

Baikov et al. (1983) and Bauer and von Kerczek (1991) carried out their research in the context of a stability analysis: that is, equations are linearized about an oscillating base flow with a uniform thickness. Inherent in this approach is the assumption that the wall oscillations do not act to create waves; rather, it is only the way in which waves grow that are affected. In many applications, however, it is desirable to consider, in addition to this growth effect, how the waves themselves *form* due to the specific disturbance impinging on the system. Thus, a wavemaker problem is often the relevant problem to consider. Since extremely small disturbances can lead to unsalable products in coating operations, a linearization approach is often sufficient to analyze their effect.

This article explicitly examines the effect of wall oscillations on the propagation of waves in the uniform film region, for *any* frequency and wavelength, in the context of the linearized wavemaker problem. Furthermore, the mechanism by which these waves are formed is investigated. We restrict our attention to a single layer and thus to surface waves, although it will be shown that at least theoretically, our results are valid for multiple layers. The approach to be taken is both experimental and theoretical.

This article first presents the linearized equations that govern wave propagation in the rectilinear flow region away from the entrance region. Then, the general solution to this system is obtained, which indicates that the oscillations do not interact with the waves in the linearized wavemaker problem. Waves propagate according to the dispersion relation for a single layer flowing down a nonoscillating incline and thus reduce to the case investigated by previous researchers cited above. The numerical solution to determine the dispersion relationship is not discussed here, since it was detailed earlier (Weinstein, 1990); only results are presented. To verify these theoretical results, experiments are performed as follows. First a baseline comparison is obtained between the theoretical dispersion relation and experiments when there are no oscillations. To this end, a technique that has been previously used to generate waves on the surface of a liquid at rest (Sohl et al., 1978) is applied to the present flow configuration; the range of wavenumbers studied by this technique is $\alpha\epsilon(0.3, 6.0)$. Next, experiments are performed when the incline is oscillating and compared with theory, thus deducing the effect of wall oscillations. The appendix demonstrates theoretically the effect of incline oscillations which are perpendicular to the incline on wave propagation.

Theory

Governing equations for the uniform film region

In this section, the linearized equations which govern wave propagation due to an oscillating incline are developed, where these equations are valid in the uniform film region (Figure 1). To this end, consider the following problem specification. A single layer of Newtonian fluid with viscosity μ is flowing down a plane inclined to the horizontal at angle γ, where the volumetric flow rate per unit width is Q. The surface of the inclined plane (the wall) itself oscillates with speed amplitude V and frequency ω', where the oscillation is in the direction of flow. Let the thickness of the uniform fluid film obtained when there are no oscillations be denoted by d. A coordinate system is chosen, where $y=\eta(x, t)$ is the location of the free surface and $y=d$ is the location of the oscillating wall; the x direction is down the incline parallel to the wall, where $x=0$ gives the location of the beginning of the uniform film region. Let P_A and ρ denote the constant atmospheric pressure and surface tension, respectively. The flow field is assumed to be two-dimensional, and thus there is no flow across the width of the incline. The goal is to determine how wave propagation is affected by the steady oscillation of the wall; the initial transients induced, when the wall motion begins, are not considered here.

The boundary condition which incorporates the effect of the oscillating wall is the no-slip condition at the wall, which in dimensionless form is given by:

$$\overline{V}_x=\epsilon e^{-i\omega\bar{t}} \quad \text{at} \quad \bar{y}=1 \tag{1}$$

where it is understood that the real part of this expression represents the physical quantity and

$$\epsilon\equiv\frac{Vd}{Q},\ \omega\equiv\frac{\omega' d^2}{Q},\ \overline{V}_x=\left(\frac{d}{Q}\right)V_x,\ \bar{y}=\frac{y}{d},\ \bar{t}=\frac{tQ}{d^2}$$

We now restrict attention to small-amplitude disturbances, that is, the case where $\epsilon\ll 1$. Thus, the solution to the wall oscillation problem can be found as a small perturbation away from the uniform flow state, where no oscillations are present and the interface is parallel to the wall. The dimensionless solution for flow down an inclined plane is given by:

$$\overline{V}_{x_0}=\frac{3}{2}(1-\bar{y}^2) \tag{2a}$$

where

$$d=\left(\frac{3Q\mu}{\rho g\sin\gamma}\right)^{1/3} \tag{2b}$$

In Eq. 2, subscript 0 denotes that a lowest-order approximation has been made, that is, no wall oscillations are seen at this order. There is no appropriate pressure scale to be used, since the pressure is simply hydrostatic and does not interact with the flow at the lowest order; the choice of this scale is made based on the linearized equations which follow. Anticipating the next order results, the lowest-order pressure has the form:

$$\overline{P}_o=\frac{3\cot\gamma}{Re}\bar{y}+\overline{P}_A,\ \text{where}\ \overline{P}=\frac{d^2}{\rho Q^2}P\ \text{and}\ Re=\frac{\rho Q}{\mu} \tag{2c}$$

This concludes consideration of the uniform flow problem.

To see the effect of the wall oscillations, the dependent variables describing the flow are perturbed about the uniform flow solution in the limit as $\epsilon\to 0$:

$$\overline{V}_x\sim\overline{V}_{x_0}(\bar{y})+\epsilon\overline{V}_{x_1}(\bar{x}, \bar{y}, \bar{t};\ Re,\ Ca,\ \gamma)+O(\epsilon^2) \tag{3a}$$

$$\overline{V}_y\sim\epsilon\overline{V}_{y_1}(\bar{x}, \bar{y}, \bar{t};\ Re,\ Ca,\ \gamma)+O(\epsilon^2) \tag{3b}$$

$$\overline{P}\sim\overline{P}_o(\bar{y};\ Re,\ \gamma)+\epsilon\overline{P}_1(\bar{x}, \bar{y}, \bar{t};\ Re,\ Ca,\ \gamma)+O(\epsilon^2) \tag{3c}$$

$$\bar{\eta}\sim\epsilon\bar{\eta}_1(\bar{x}, \bar{t};\ Re,\ Ca,\ \gamma)+O(\epsilon^2) \tag{3d}$$

where

$$\overline{V}_y=\left(\frac{d}{Q}\right)V_y,\ \bar{\eta}=\frac{\eta}{d},\ \text{Ca}=\frac{\mu Q}{d\sigma},\ \bar{x}=\frac{x}{d}$$

Note that Eq. 3d indicates that the amplitude of the surface waves is assumed to be of the same order as the amplitude of the plate oscillation. Substituting the expansions (Eq. 3) into the full Navier-Stokes equations, continuity equation, and appropriate boundary conditions (including Eq. 1) and retaining terms only to $O(\epsilon)$, the results are:

Continuity:

$$\frac{\partial\overline{V}_{x_1}}{\partial\bar{x}}+\frac{\partial\overline{V}_{y_1}}{\partial\bar{y}}=0 \tag{4a}$$

Navier-Stokes:

$$Re\left(\frac{\partial\overline{V}_{x_1}}{\partial\bar{t}}+\overline{V}_{x_0}\frac{\partial\overline{V}_{x_1}}{\partial\bar{x}}+\overline{V}_{y_1}\frac{\partial\overline{V}_{x_0}}{\partial\bar{y}}\right)$$
$$=-\frac{\partial\overline{P}_1}{\partial\bar{x}}+\left(\frac{\partial^2\overline{V}_{x_1}}{\partial\bar{x}^2}+\frac{\partial^2\overline{V}_{x_1}}{\partial\bar{y}^2}\right) \tag{4b}$$

$$Re\left(\frac{\partial \overline{V}_{y_1}}{\partial \bar{t}}+\overline{V}_{x_0}\frac{\partial \overline{V}_{y_1}}{\partial \bar{x}}\right)=-\frac{\partial \overline{P}_1}{\partial \bar{y}}+\left(\frac{\partial^2 \overline{V}_{y_1}}{\partial \bar{x}^2}+\frac{\partial^2 \overline{V}_{y_1}}{\partial \bar{y}^2}\right) \quad (4c)$$

Kinematic and no-slip boundary conditions at wall:

$$\overline{V}_{y_1}=0 \quad \text{at} \quad \bar{y}=1 \quad (4d)$$

$$\overline{V}_{x_1}=e^{-i\omega \bar{t}} \quad \text{at} \quad \bar{y}=1 \quad (4e)$$

Kinematic boundary condition at interface:

$$\overline{V}_{y_1}=\frac{\partial \overline{\eta}_1}{\partial \bar{t}}+\overline{V}_{x_0}\frac{\partial \overline{\eta}_1}{\partial \bar{x}} \quad \text{at} \quad \bar{y}=0 \quad (4f)$$

Dynamic boundary conditions at interface:

$$\overline{P}_1+\frac{3\cot\gamma}{Re}\overline{\eta}_1-\frac{2}{Re}\frac{\partial \overline{V}_{y_1}}{\partial \bar{y}}-\frac{1}{CaRe}\frac{\partial^2 \overline{\eta}_1}{\partial \bar{x}^2}=0 \quad \text{at} \quad \bar{y}=0 \quad (4g)$$

$$\frac{\partial \overline{V}_{x_1}}{\partial \bar{y}}+\frac{\partial \overline{V}_{y_1}}{\partial \bar{x}}=-\frac{\partial^2 \overline{V}_{x_0}}{\partial \bar{y}^2}\overline{\eta}_1 \quad \text{at} \quad \bar{y}=0 \quad (4h)$$

No conditions are required as $\bar{x}\to\infty$, since it is anticipated that waves can grow freely if the waves remain linear and the incline is long enough. Furthermore, no conditions are supplied at $\bar{t}=0$, since transient effects are not to be investigated. The solution to Eqs. 4 gives the behavior of the flow in the uniform film region of the incline (for large $\bar{x}$ in Figure 1). The general solution to this system is discussed next.

Wave Solutions in the Uniform Film Region

A solution to the system of Eqs. 4 is accomplished by utilizing the following superposition:

$$\overline{V}_{x_1}=\overline{F}(\bar{y},\bar{t})+\tilde{V}_{x_1}(\bar{x},\bar{y},\bar{t}) \quad (5a)$$

$$\overline{V}_{y_1}=\tilde{V}_{y_1}(\bar{x},\bar{y},\bar{t}) \quad (5b)$$

$$\overline{P}_1=\tilde{P}_1(\bar{x},\bar{y},\bar{t}) \quad (5c)$$

$$\overline{\eta}_1=\tilde{\eta}_1(\bar{x},\bar{t}) \quad (5d)$$

Equations 5a–5d are substituted into Eqs. 4a–4h, and the following boundary-value problem for $\overline{F}$ is obtained:

$$Re\frac{\partial \overline{F}}{\partial \bar{t}}=\frac{\partial^2 \overline{F}}{\partial \bar{y}^2} \quad (6a)$$

$$\overline{F}=e^{-i\omega \bar{t}} \quad \text{at} \quad \bar{y}=1 \quad (6b)$$

$$\frac{\partial \overline{F}}{\partial \bar{y}}=0 \quad \text{at} \quad \bar{y}=0 \quad (6c)$$

The solution to the system of Eqs. 6 yields:

$$\overline{F}=\frac{\cosh((1-i)\beta\bar{y})}{\cosh((1-i)\beta)}e^{-i\omega \bar{t}} \quad (7)$$

where i denotes the pure imaginary number, and

$$\beta=\sqrt{\frac{\omega Re}{2}}$$

The remaining boundary-value problem for those variables denoted with a tilde ($\sim$) is identical to the system of Eq. 4, where the tilde replaces the overbar on the dependent variables and the condition 4e is replaced with:

$$\tilde{V}_{x_1}=0 \quad \text{at} \quad \bar{y}=1 \quad (8)$$

The system of Eqs. 4, using condition 8, will be referred to as the tilde system. The solution to this system can be facilitated by defining a stream function, $\tilde{\Psi}$, which automatically satisfies Eq. 4a and removes the explicit dependence of the pressure in Eqs. 4, where

$$\tilde{V}_{x_1}=\frac{\partial \tilde{\Psi}}{\partial \bar{y}}, \quad \tilde{V}_{y_1}=-\frac{\partial \tilde{\Psi}}{\partial \bar{x}} \quad (9)$$

These quantities are substituted into the above equations, and an equivalent boundary-value problem to solve for $\tilde{\Psi}$ is obtained. All solutions to the tilde system can be written as the superposition of traveling waves of the form:

$$\tilde{\Psi}=\tilde{\psi}(\bar{y})e^{i(\alpha\bar{x}-\theta\bar{t})} \quad (10a)$$

$$\tilde{\eta}_1=He^{i(\alpha\bar{x}-\theta\bar{t})} \quad (10b)$$

where it is necessary to determine the unknown function $\tilde{\psi}(\bar{y})$, the unknown constant H, and the functionality $\alpha(\theta)$. In Eqs. 10, i denotes imaginary, θ is a dimensionless real frequency, $\alpha=\alpha_R+i\alpha_I$ is the complex wavenumber, where the real part is defined as $\alpha_R=2\pi d/\lambda$ (λ is the wavelength), and the imaginary part, denoted by α_I, determines the spatial growth or decay of waves along the inclined plane. In this article, we call $-\alpha_I$ the growth factor, where if $-\alpha_I$ is positive there is wave growth; if $-\alpha_I$ is negative there is wave damping. A spatial formulation of the stability problem has been chosen here, since this type of growth is typically exhibited on an incline (see Krantz and Owens, 1973; Weinstein, 1990).

Substituting Eqs. 10 into the kinematic boundary condition at the interface (Eq. 4f), the constant H in Eq. 10b can be related to $\tilde{\psi}(0)$ as:

$$H=\frac{\alpha\tilde{\psi}(0)}{\theta-\alpha\overline{V}_{x_0}(0)} \quad (11)$$

Then, using Eq. 11, a boundary-value problem is obtained only in terms of the unknown function $\tilde{\psi}(\bar{y})$ as well as the complex wavenumber α. The Navier-Stokes equations (Eqs. 4b and 4c) become:

$$\frac{d^4\tilde{\psi}}{d\bar{y}^4}-2\alpha^2\frac{d^2\tilde{\psi}}{d\bar{y}^2}+\alpha^4\tilde{\psi}=iRe\left[(\alpha\overline{V}_{x_0}-\theta)\left(\frac{d^2\tilde{\psi}}{d\bar{y}^2}-\alpha^2\tilde{\psi}\right)-\alpha\tilde{\psi}\frac{d^2\overline{V}_{x_0}}{d\bar{y}^2}\right] \quad (12a)$$

The no-slip and kinematic conditions Eqs. 4d and 8 become:

$$\begin{pmatrix} \tilde{\psi}=0 \\ \dfrac{d\tilde{\psi}}{d\bar{y}}=0 \end{pmatrix} \quad \text{at} \quad \bar{y}=1 \tag{12b,c}$$

while the dynamic normal and tangential components of the dynamic boundary conditions (Eqs. 4g and 4h) become:

$$\frac{d^3\tilde{\psi}}{d\bar{y}^3}+(iRe[\theta-\alpha\overline{V}_{x_0}]-3\alpha^2)\frac{d\tilde{\psi}}{d\bar{y}} + \left(3\cot\gamma+\frac{\alpha^2}{Ca}\right)\frac{i\alpha^2\tilde{\psi}}{(\theta-\alpha\overline{V}_{x_0})}=0 \quad \text{at} \quad \bar{y}=0 \tag{12d}$$

$$\frac{d^2\tilde{\psi}}{d\bar{y}^2}+\alpha^2\tilde{\psi}+\frac{d^2\overline{V}_{x_0}}{d\bar{y}^2}\frac{\alpha\tilde{\psi}}{(\theta-\alpha\overline{V}_{x_0})}=0 \quad \text{at} \quad \bar{y}=0 \tag{12e}$$

The system of Eqs. 12 constitutes a nonlinear eigenvalue problem to solve for the complex eigenfunction $\tilde{\psi}(\bar{y})$ and the eigenvalue α, for given θ, geometrical, fluid, and flow properties. The solution for $\tilde{\psi}(\bar{y})$ is determined to be an arbitrary multiplicative constant due to the indeterminate nature of an eigenvalue system. Thus each solution for $\tilde{\Psi}$ and $\tilde{\eta}_1$, given by Eq. 10 for a particular θ, can be superimposed to obtain a general solution for any disturbance. Thus, the general solution for the stream function, denoted as $\tilde{\Psi}_u$, is given by:

$$\tilde{\Psi}_u=\sum_\theta A_\theta\tilde{\psi}(\bar{y};\theta)e^{i[\alpha(\theta)\bar{x}-\theta\bar{t}]} \tag{13}$$

where A_θ's are the set of unknown constants referred to above, being functions of θ. In Eq. 13, the fact that $\tilde{\psi}$ and α depend on θ has been indicated. This completes the solution to the tilde problem.

Finally, the most general interface solution for the system of Eqs. 4 can be written using Eqs. 5d, 10b, 11 and 13 as:

$$\bar{\eta}_{1_u}=\sum_\theta A_\theta\frac{\alpha(\theta)\tilde{\psi}(0;\theta)}{[\theta-\alpha(\theta)\overline{V}_{x_0}(0)]}e^{i[\alpha(\theta)\bar{x}-\theta\bar{t}]} \tag{14a}$$

while the most general velocity solutions for the system of Eqs. 4 are written using Eqs. 5a, 5b, 7, 9 and 13:

$$\overline{V}_{x_{1_u}}=\text{Real}\left[\frac{\cosh[(1-i)\beta\bar{y}]}{\cosh[(1-i)\beta]}e^{-i\omega\bar{t}}\right] + \sum_\theta A_\theta\frac{d\tilde{\psi}}{d\bar{y}}e^{i[\alpha(\theta)\bar{x}-\theta\bar{t}]} \tag{14b}$$

$$\overline{V}_{y_{1_u}}=-\sum_\theta i\alpha(\theta)A_\theta\tilde{\psi}(\bar{y};\theta)e^{i[\alpha(\theta)\bar{x}-\theta\bar{t}]} \tag{14c}$$

where the subscript u has been added to denote that Eqs. 14 are valid only in the uniform film region. At this point, the constants A_θ are unknown. These unknown constants arise since only the behavior in the uniform film region has been considered; no attention has been given to the wave behavior in the vicinity of the entrance region. These constants are evaluated in the context of experimental results presented later.

The physical meaning of the results given in Eqs. 14 is now discussed. In Eq. 14b, the first term in the brackets is the particular solution that incorporates the effect of the wall oscillation. This term does not provide any traveling wave contribution to the velocity. On the other hand, the summation terms (the contribution from the tilde problem) in Eqs. 14 show no effect of the wall oscillation (see boundary condition 8), but do have traveling waves. Only the traveling wave solution is present for the interface shape in Eq. 14a. It thus appears as if the interface shape is not affected at all by the wall oscillation. This is an interesting result, since it might be expected that there is some frequency at which a certain wave or group of waves would continually absorb energy from the oscillation. The result (Eq. 14a) indicates that the waves do not gain energy due to the wall oscillation as the fluid flows down the incline. *Furthermore, the way in which the wave grows is not determined by the wall oscillation, since the eigensystem solved (the tilde problem) is identical to that of the single-layer references cited in the introduction, where no particular initial disturbance was considered.* It should be noted here that, when the wall is oscillating perpendicular to the plane of inclination, a similar theoretical structure arises (see the Appendix).

The experimental verification of the above theory and physical interpretation is discussed subsequently. The system of Eqs. 12, which is solved earlier (Weinstein, 1990), determines the dispersion relation that governs wave propagation. Comparisons between theoretical and experimental results are presented after the following description of the experimental technique and apparatus.

Experimental Technique and Apparatus

Wave propagation measurements were obtained on a stainless steel plane, inclined at an angle 15° to the horizontal, which was 10 cm wide and 14 cm long. The plane itself was jacketed so that the temperature in the experiment could be maintained at 23.5°C; in addition, the inclined plane apparatus was placed on an air table to isolate our experiments from room vibrations. The flow rate was maintained by a gear pump, where a widthwise constant-layer thickness on the incline was achieved by delivering the fluid through a narrow slot (as shown in Figure 1, where the incline extends widthwise into the figure). An air chamber was placed in the delivery line to damp pressure fluctuations due to the gear pump. At the end of the incline, the liquid effluent was collected and was recycled back into the system. To adjust viscosities in our experiments, we used mixtures of deionized water, glycerol (98% purity), and blue dye; this dye was checked to make sure it was not surface-active. The viscosity was measured with a Couette viscometer.

The wave detection system used was described fully by Sohl et al. (1978), and so only the most relevant details are presented here. Wave measurements were made by reflecting a He-Ne laser beam off the surface of the flowing liquid and trapping the reflected light with a sensing diode; the blue dye that was added to our fluids absorbed the transmitted part of the beam. The theory behind the detection of the reflected light is as follows. For a traveling wave of dimensional frequency and complex wavenumbers given by ω' and α', respectively, the

amplitude of a wave, A, is given in terms of a reference amplitude, A_0, by:

$$A = A_0 e^{i(\omega' t - \alpha' x)} \tag{15a}$$

The detector gives an output voltage signal, S, which is proportional to the local slope of the surface, which is given in terms of Eq. 15a as:

$$S = -(2rDi\alpha')A \tag{15b}$$

In Eq. 15b, r is the gain of the detector and D is the mean distance of the detector from the fluid surface. Thus, the evolution of the output signal according to time and distance follows the same exponential law as for the thickness fluctuations induced by a wave. Through use of a lock-in amplifier, which integrates the time-dependent sinusoidal variations according to Eq. 15, the measurement of both the modulus and phase of the detected signal as a function of position along the incline can be obtained. The precise positioning of the detector was computer-controlled. The output voltage of the lock-in amplifier is digitized and then processed by a computer. A curve-fitting program is used to extract the growth factor, $-\alpha_I$, and the wavelength, through α_R, for a particular frequency wave.

The wave-detection scheme just described has a high sensitivity and is particularly suitable to small-amplitude waves regardless of the growth. In spite of the high sensitivity of the device, measurements were not possible for $\alpha_R < 0.3$, because slope variations were too low to be detected. The limit for the detection for high wavenumbers was reached when the half wavelength was smaller than the width of the laser beam at the surface. For these reasons, the practical frequency range of detection in our experiments was 10 to 600 Hz. In contrast to the work of Krantz and Goren (1971), the described laser measurement technique does not yield a direct measurement of the amplitude of the film thickness variations, since only slope is measured. Nevertheless, the wave amplitude can be calculated by the knowledge of the complex wavenumber and measured voltages according to Eqs. 15. It should be noted here that Jones and Whitaker (1966) used a different detector device which was also sensitive to slope.

For experiments where the wall was motionless, an experimental method called electrocapillarity was used to excite the free surface of the liquid. This technique is described extensively by Sohl et al. (1978). Although Sohl et al. used this technique to study waves on the surface of a *stagnant liquid* crystal, we did not find any particular problems in applying this technique to a *flowing liquid*. To apply the electrocapillarity technique, a sharp metallic blade, configured lengthwise perpendicular to the flow, was placed in close proximity to the fluid surface; the distance between the fluid and the blade was about 1 mm. An electrical field was induced between the liquid and the blade which caused the surface to rise in the vicinity of the blade. It should be noted that, because the electrical force was only attractive and was insensitive to the directionality of the electrical field, the surface moved at twice the voltage frequency. This technique was capable of creating measurable waves with frequencies up to the limit of the detection device itself, that is, 600 Hz.

The major advantage of the electrocapillarity technique is that it does not disturb the fluid flow as does a mechanical exciter (such as that used by Krantz and Goren, 1971), since the liquid is not contacted by the blade. This is particularly important in the systems which are studied here, since high-wave damping is exhibited for many wavelengths; thus, it is necessary to examine waves in the vicinity of the exciter itself to obtain measurable amplitudes. If the fluid flow were radically disturbed by the exciter, then wave measurements would not be representative of propagation along a uniform layer; the underlying disturbed fluid flow would affect the wave propagation itself.

To study the effect of wall oscillations on the wave propagation, a Bruel and Kjaer shaker (type 4809) was used to exert a sinusoidal force against the inclined plane. The incline was then constrained to move in the flow direction by steel beams which flexed primarily in the direction of the applied force. The experimental apparatus was tested in vibration, and it had a resonance at 30 Hz. Around this resonant frequency, from 10 Hz to 80 Hz, the ratio between the amplitude of the oscillation parallel to the flow and that perpendicular to the flow is above 20. Thus, it is in this frequency range that measurements were taken. The detection device previously described was kept fixed in the lab frame when the inclined plane was oscillated. In either type of experiment, care was taken to assure that the detected waves were linear. This was accomplished by increasing or decreasing the source level of disturbance and verifying that the wave amplitudes according to Eqs. 15 increased or decreased proportionately to the source.

Results and Discussion

We first present the wave propagation results obtained for a nonoscillating wall, where waves were excited using the electrocapillarity technique. To this end, four experimental conditions were investigated, whose fluid and flow properties are summarized in Table 1. Also shown in this table is the uniform fluid thickness for each condition calculated from Eq. 2b. Based on the stability criterion derived by Benjamin (1957), the flow will be unstable when $Re > 5\cot\gamma/6$; for our experiments, the critical Reynolds number is 3.11. Conditions 1 to 3 have Reynolds numbers larger than this value and are un-

Table 1. Summary of Experimental Conditions

Condition	μ (poise)	ρ (g/cm^3)	σ (dyne/cm)	Q (cm^2/s)	d (cm)	ϵ
1	0.031	1.08	70	0.8	0.065	7.0×10^{-3}–3.1×10^{-2}
2	0.060	1.11	68	0.8	0.080	9.0×10^{-3}–4.4×10^{-2}
3	0.095	1.15	66	0.5	0.079	1.8×10^{-2}–7.2×10^{-2}
4	0.175	1.17	65	0.5	0.096	1.9×10^{-2}–1.4×10^{-1}
5	0.380	1.20	64	0.5	0.123	3.3×10^{-2}–2.6×10^{-1}

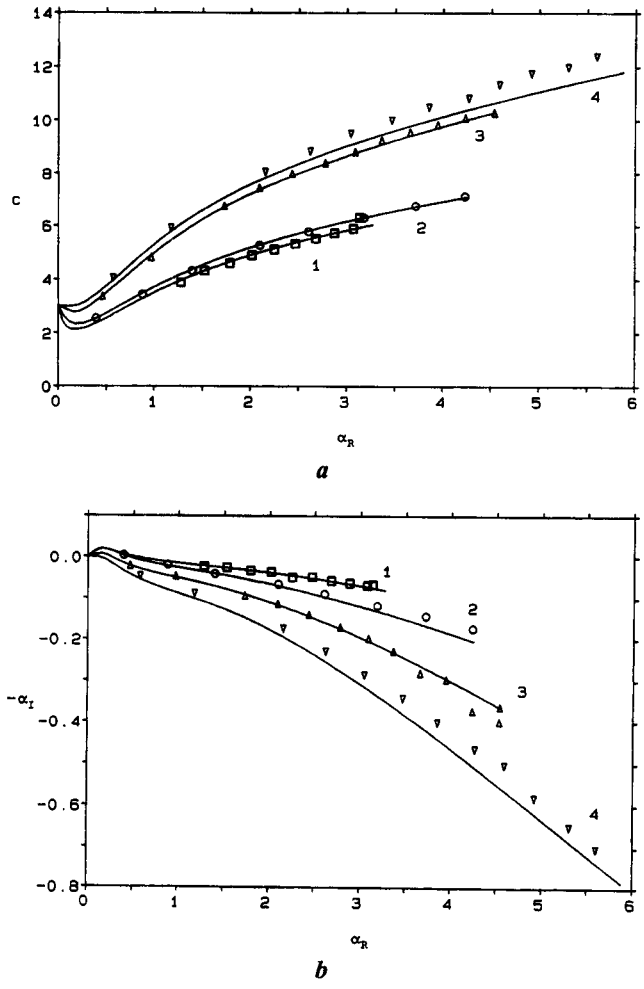

Figure 2. Dimensionless comparison of theoretical wave propagation and experimental electrocapillarity results: (a) wave speeds; (b) wave growth.

Experimental results: condition 1, □; condition 2, ○; condition 3, △; condition 4, ▽. Corresponding theoretical results are given by solid lines labeled by condition number.

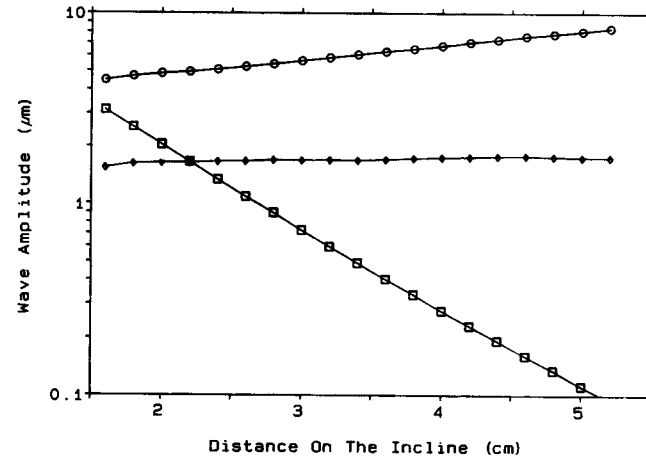

Figure 3. Typical experimental spatial evolution of the wave amplitude (dimensional).

Condition 1 at 20 Hz, ○; condition 1 at 40 Hz, ◇; condition 5 at 20 Hz, □.

stable on the inclined plane, while condition 4 has a Reynolds number close to the critical value. Figure 2a gives a dimensionless comparison between the theoretical and experimental wave speed, C, as a function of the wavenumber, α_R, for the four conditions. Due to the experimental limitations of our detection device, we could not measure wavenumbers less than approximately 0.3. Thus, the experimental wave speeds are always found to increase as shown in Figure 2a. Figure 2b gives a similar comparison of the experimental and dimensionless theoretical spatial growth factors, $-\alpha_I$, as a function of α_R. The typical scatter in the experimental data was within the size of the plot symbols shown in the figures. The agreement between theory and experiment is quite good.

Next, the electrocapillarity excitation was switched off, and the wall was oscillated at various discrete frequencies for the same four conditions; as before, wave speeds and wave growths were measured. In addition, a fifth condition, described in Table 1, was also studied. The range of dimensionless wall oscillations (the range of ϵ values) used to obtain results for each condition is indicated in Table 1. Despite the relatively large values of ϵ for conditions 4 and 5, the amplitude of the waves were found to vary linearly with the amplitude of the oscillation. It was always observed that waves were formed having the same frequency as the wall oscillation. Figure 3 shows the typical evolution of the dimensional wave amplitude (related to the measured detector voltage by Eq. 15) as a function of the distance on the plane for condition 1 when the wall is oscillated at frequencies of 20 Hz and 40 Hz, and for condition 5 for a wall oscillation of 20 Hz. These results indicate that waves grow or decay exponentially in distance. Figure 4a gives the dimensionless comparison between experimental and theoretical wave speeds for the five conditions; Figure 4b gives the same comparisons for wave growth. As in the case of electrocapillarity disturbances; the theoretical and experimental results agree quite well.

We now comment on the apparent systematic errors found for cases of high spatial damping, for both the electrocapillarity and wall oscillation excitations. In particular, a systematic error is seen in Figures 2a and 2b for condition 4 (electrocapillarity excitation), and a similar error is found in Figures 4a and 4b for conditions 4 and 5 (wall oscillation excitation). The likely common source of this error is due to the detection device itself. In particular, the high damping for these conditions led to extremely small wave amplitudes which caused very small output signals from our detector. The systematic errors are likely a manifestation of the measurement limitations of the detection device.

The experimental results obtained with an oscillating wall agree with the theory, as do the results obtained using electrocapillarity. This demonstrates that waves propagate as if the wall were not oscillating at all. Despite this fact, the experimental results also show that the waves are formed having the same frequency as that of the oscillating wall. *It is thus deduced that the particular wave frequency and amplitude observed in the uniform region must be induced by the flow in the entrance region to the incline.* Then, as the fluid asymptotically approaches its uniform film solution away from the entrance region to the incline, $\bar{x} \to \infty$, wall oscillations no longer affect the waves which were already formed in the entrance

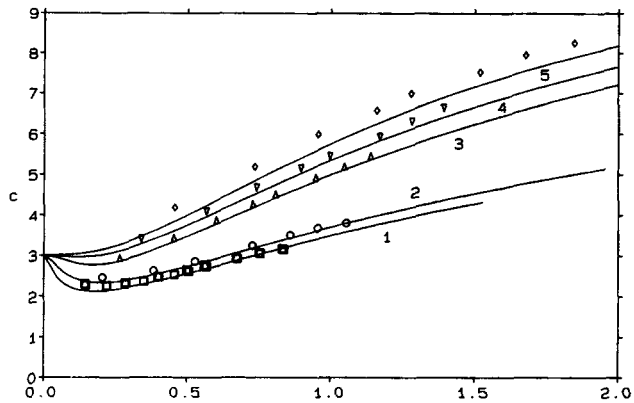

a

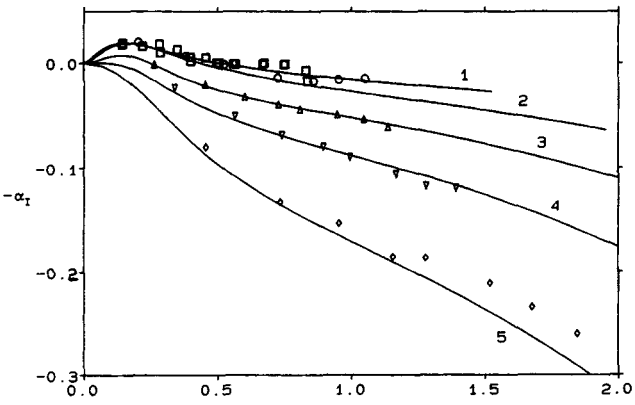

b

Figure 4. Dimensionless comparison of theoretical wave propagation and experimental wall-oscillation results: (a) wave speeds; (b) wave growth.

Experimental results: condition 1, □; condition 2, ○; condition 3, △; condition 4, ▽; condition 5, ◇; corresponding theoretical results are given by solid lines labeled by condition number.

region (see Figure 1). Furthermore, our experimental results indicate that, when waves detected in the uniform film region are of a linear nature, then the physics of the entrance region is also linear. Using this result, the selection of a particular frequency is anticipated mathematically since, if the entrance region governing equations are linearized, the time derivates indicate that Ψ in this region must have the following dependence to be consistent with the oscillating wall boundary condition (Eq. 4e):

$$\Psi = G(\bar{x}, \bar{y})e^{-i\omega\bar{t}} \tag{16a}$$

Focusing on the interface solution (Eq. 14a), then, it is clear that, for a given frequency of oscillation, only one mode is excited in the uniform film region; the only nonzero value of A_θ occurs when $\theta = \omega$, and Eq. 14a can be rewritten as:

$$\bar{\eta}_{1_\omega} = A_\omega \frac{\alpha(\omega)\bar{\psi}(0;\omega)}{(\omega - \alpha(\omega)\bar{V}_{x_0}(0))} e^{i[\alpha(\omega)\bar{x} - \omega\bar{t}]} \tag{16b}$$

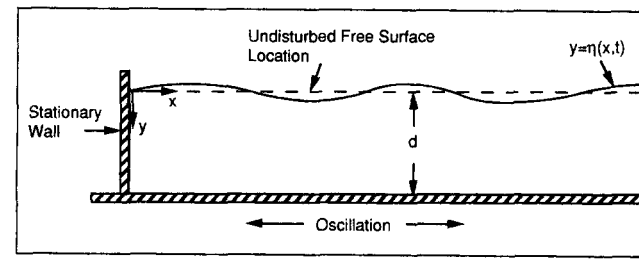

Figure 5. Geometry of the simplified model problem.

The numerical value of A_ω, giving the amplitude of the wave as $\bar{x} \to 0$, is determined by the specific physics of the entrance region. In Eq. 16b, the wavelength and wave growth, given respectively by the real and imaginary parts of α, satisfy the dispersion relation for the nonoscillating wall, but α is evaluated at the frequency ω. It should be noted, however, that other modes with different frequencies in Eq. 14a might be excited by other disturbances impinging on the system (in the uniform film and entrance region); care has been taken in experiments that wave amplitudes are large enough to overwhelm this noise.

We now discuss why the uniform film region does not affect the wave propagation, while at the same time the entrance region can induce a wave to form with a given frequency and amplitude. To this end, consider a simpler physical configuration than that of the inclined plane flow; that of waves generated in a semiinfinite trough, where the bottom wall is oscillating horizontally with a small amplitude, and at $x = 0$, there is a stationary vertical wall (see Figure 5). In this problem, the basic fluid flow is at rest, where the undisturbed thickness of the layer is given by d. Under these circumstances, the equations derived previously are valid, once the uniform flow velocity is set to zero: $\bar{V}_{x_0} = 0$. The superposition given by Eq. 5 is valid for this simplified system, and consequently, the general results given by Eq. 14 and 16 are valid, where it is understood that the dispersion relation in Eq. 16b for $\alpha(\omega)$ differs from that due to flow down an incline, since Eqs. 12 are now solved with $\bar{V}_{x_0} = 0$. (This dispersion relationship is given for a trough of infinite depth in Lamb, 1932.) Physically, near $x = 0$, as the bottom wall drags fluid toward the vertical wall, fluid must be displaced upward to conserve mass. Consequently, the horizontal motion of the wall induces a perpendicular motion of the interface. The efficiency of this motion in exciting a wave is determined by the particular frequency with which the horizontal wall oscillates. As x increases, the flow does not need to respond as readily to the vertical wall, since the interface has already deformed in the direct vicinity of the vertical wall in a local effort to conserve mass. As $x \to \infty$, the interface does not need to adjust at all to the influence of the vertical wall, and the waves which were formed near $x = 0$ then travel as if the wall is not oscillating at all.

Using the intuition from the above simplified problem, the boundary conditions in the vicinity of the entrance to the incline afford the means by which the horizontal motion of the wall induces a perpendicular motion of the interface relative to the wall. In the uniform film region, there is no boundary against which the fluid flow can readjust, and thus there is no asymmetry in the flow such that wall oscillations can translate into vertical interface distortions. Thus, there is no way for different points along the interface to gain a relative motion due to the

oscillations of the bottom wall, and thus waves cannot form in this region.

The above conclusions are consistent with the long-wavelength *stability* analyses of Bauer and von Kerczek (1991) and Baikov et al. (1983), once these are interpreted in the context of the linearized wavemaker problem. As $\epsilon \to 0$, one can interpret the oscillation effect in their analyses as being shifted to the $O(\epsilon)$ problem, despite the fact that the oscillations are incorporated into the base flow. Both of these analyses indicate that there is an $O(\epsilon^2)$ effect on *temporal* wave growth due to wall oscillations at long wavelengths. Note, however, that the functional form for the solution of the wavemaker problem, given by Eq. 16a, indicates that only *spatial* growth is possible. The transformation of Gaster (1962) is thus employed to relate the temporal and spatial growth rates in the long wavelength limit; it is straightforward to show that there is an $O(\epsilon^2)$ effect of the oscillations on *spatial* wave growth. It is reasonable to expect that this asymptotic ordering in ϵ would not change for finite wavelengths.

The above described physics appears to be valid for the case of wall oscillations perpendicular to the plane of the incline, based on the theory in the Appendix. Furthermore, although it is not presented in this article, the presented theory can be easily generalized to the case of multiple-layer flow down an oscillating inclined plane. In particular, in the uniform film region, it is possible to superimpose two solutions: one incorporates all of the oscillations, but the interfaces are flat; the other gives the wave propagation on a stationary inclined surface. Thus, it would appear that the physics reported here is valid for multiple-layer flows as well. In contrast to the single-layer systems investigated here, however, the largest growing waves in multiple-layer systems will typically arise at much larger wave numbers, as discussed in the Introduction.

Summary and Conclusions

The propagation of surface waves has been investigated theoretically and experimentally for the case of a single layer of viscous liquid flowing down an inclined plane, where the plane is oscillating in the flow direction. This work has focused on the linearized wavemaker problem, where the oscillations create waves that are small perturbations from the undisturbed flow. Both theoretical and experimental means have been used to deduce the propagation characteristics of the waves. To this end, experiments were first performed where the incline was motionless to establish a baseline comparison between theory (Weinstein, 1990) and our experiments; then, experiments were performed when the incline was oscillating. In either case, there was good agreement between experiment and the theory.

Experiments confirm that in the uniform film region, wall oscillations do not interact with waves which travel along the free surface. These waves grow as if there were no oscillation at all; their propagation is governed by a dispersion relation among frequency, wavelength, and wave growth for single-layer flow down a nonoscillating inclined plane. Alternatively, the entrance region to the incline is responsible for exciting the various wave frequencies which are observed down the incline, as well as the initial energy imparted to these waves. The boundary conditions in the vicinity of the entrance to the incline afford the means by which the horizontal motion of the wall can induce a perpendicular motion of the interface relative to the wall; this motion leads to the formation of waves. In the uniform film region, there is no boundary against which the fluid flow can readjust, and thus there is no asymmetry in the flow such that wall oscillations can translate into vertical interface distortions; consequently, wall oscillations do not interact with the waves which propagate through this region. These conclusions are expected to be valid when there are oscillations perpendicular to the incline, as well as for the case of multiple stacked layers.

Notation

Ca = capillary number, $Ca \equiv \mu Q/\sigma d$
d = film thickness
g = gravitational constant
H = complex amplitude of surface wave
i = imaginary number
P = pressure
P_A = atmospheric pressure
Q = flow rate per unit width
Re = Reynolds number, $Re \equiv \rho Q/\mu$
t = time
V = amplitude of wall vibration
V_x = velocity in the x direction
V_y = velocity in the y direction
x, y = spatial variables

Greek letters

α = dimensionless complex wavenumber
α_I = imaginary part of α, yielding spatial growth information
α_R = real part of α, where $\alpha_R \equiv 2\pi d/\lambda$
β = dimensionless vibration number, $\beta \equiv \sqrt{\omega Re/2}$
ϵ = dimensionless vibration parameter, $\epsilon \equiv \sqrt{Vd/Q}$
γ = angle of inclination
η = location of free surface
λ = wavelength
μ = viscosity
θ = dimensionless frequency
ρ = density
σ = surface tension
ω = dimensionless frequency of wall oscillation
ω' = dimensional frequency of wall oscillation
$\psi(y)$ = y-dependent component of stream function
Ψ = stream function

Subscripts

0 = lowest order, $O(1)$
1 = first order, $O(\epsilon)$
u = uniform film region, most general solution

Superscripts

$\bar{}$ = dimensionless
$\tilde{}$ = dimensionless, without vibrations

Literature Cited

Akhtaruzzaman, A. F. M., C. K. Wang, and S. P. Lin, "Wave Motion in Multilayered Liquid Films," *J. Appl. Mech.*, **45**, 25 (1978).

Baikov, V. I., A. T. Listrov, and Z. A. Shabunina, "Stability of Film Flowing Down Along an Oscillating Surface," *J. Eng. Phys.*, **43**(6), 1413 (1983).

Bauer, R. J., and C. H. von Kerczek, "Stability of Liquid Film Flow Down an Oscillating Wall," *Trans. ASME*, **58**, 278 (1991).

Baumlin, J. M., and A. Pasquet, "Flow Stability on an Inclined Plane: Modeling and Experimental Results," AIChE Meeting, Int. Symp. of Thin-Film Coating, Paper 5b, New Orleans (1988).

Benjamin, T. B., "Wave Formation in Laminar Flow Down an Inclined Plane," *J. Fluid Mech.*, **2**, 554 (1957).

Binnie, A. M., "Experiments on the Onset of Wave Formation on a

Film of Water Flowing Down a Vertical Plane," *J. Fluid Mech.*, **2**, 551 (1957).
Gaster, M., "A Note on the Relation between Temporally-Increasing and Spatially-Increasing Disturbances in Hydrodynamic Stability," *J. Fluid Mech.*, **14**, 222 (1962).
Jones, L. O., and S. Whitaker, "An Experimental Study of Falling Liquid Films," *AIChE J.*, **12**(3), 525 (1966).
Kao, T. W., "Stability of Two-Layer Viscous Stratified Flow Down an Inclined Plane," *Phys. Fluids*, **8**(5), 812 (1965a).
Kao, T. W., "Role of the Interface in the Stability of Stratified Flow Down an Inclined Plane," *Phys. Fluids*, **8**(12), 2190 (1965b).
Kao, T. W., "Role of Viscosity Stratification in the Stability of Two-Layer Flow Down an Incline," *J. Fluid Mech.*, **33**, 561 (1968).
Krantz, W. B., and S. L. Goren, "Stability of Thin Liquid Films Flowing Down an Incline," *Ind. Eng. Chem. Fund.*, **10**(1), 91 (1971).
Krantz, W. B., and W. B. Owens, "Spatial Formulation of the Orr-Sommerfeld Equation for Thin Liquid Films Flowing Down a Plane," *AIChE J.*, **19**(6), 1163 (1973).
Lamb, H., *Hydrodynamics*, 6th ed., Cambridge University Press, 625 (1932).
Loewenherz, D. S., and C. J. Lawrence, "The Effect of Viscosity Stratification on the Stability of a Free Surface Flow at Low Reynolds Number," *Phys. Fluids A*, **1**(10), 1686 (1989).
Sohl, C. H., K. Miyano, and J. B. Ketterson, "Novel Technique for Dynamic Surface Tension and Viscosity Measurements at Liquid-Gas Interfaces," *Rev. Sci. Instrum.*, **49**(10), 1464 (1978).
Wang, C. K., J. J. Seaborg, and S. P. Lin, "Instability of Multi-Layered Liquid Films," *Phys. Fluids*, **21**(10), 1669 (1978).
Weinstein, S. J., "Wave Propagation in the Flow of Shear-Thinning Fluids Down an Incline," *AIChE J.*, **36**(12), 1873 (1990).
Yih, C., "Stability of Liquid Flow Down an Inclined Plane," *Phys. Fluids*, **6**(3), 321 (1963).

Appendix: Effect of Oscillations Perpendicular to the Wall in the Uniform Film Region

We now consider the case where the oscillations of the wall are perpendicular to the plane of the incline. It is shown that this new problem has the same general mathematical structure as that of the previous problem. That is, away from the entrance region to the incline, the perpendicular oscillations have no effect on wave propagation. As in the case where oscillations occur in the flow direction, the entrance region to the incline appears to be where the initial wave amplitude and wave frequency are determined when there are perpendicular incline oscillations.

The boundary condition which incorporates the effect of a wall oscillating with a displacement amplitude, b, is the kinematic condition at the wall:

$$\bar{V}_y = \epsilon\omega e^{-i\omega\bar{t}} \quad \text{at} \quad \bar{y} = 1 + i\epsilon e^{-i\omega\bar{t}} \tag{A1}$$

where

$$\epsilon \equiv \frac{b}{d}$$

As in the case where oscillations occur in the flow direction, we will assume that the parameter ϵ is small; thus, the solution to the oscillation problem can be found as a small perturbation away from the uniform flow state given by Eq. 2. Thus, the dependent variables are perturbed as in Eq. 3, where it is understood that the parameter ϵ now has a different meaning. The expansions (Eq. 3) are substituted into the full Navier-Stokes equations, continuity equation, and boundary conditions, and terms are retained only to $O(\epsilon)$. The linearized equations are given by Eq. 4, where the kinematic and no-slip conditions at the plate surface, given respectively by Eqs. 4d and 4e, are replaced for the new problem with:

$$\bar{V}_{y_1} = \omega e^{-i\omega\bar{t}} \quad \text{at} \quad \bar{y} = 1 \tag{A2a}$$

$$\bar{V}_{x_1} = -i\frac{d\bar{V}_{x_0}}{d\bar{y}} e^{-i\omega\bar{t}} \quad \text{at} \quad \bar{y} = 1 \tag{A2b}$$

No conditions are required as $\bar{x} \to \infty$, since it is anticipated that waves can grow freely as long as the incline is long enough; furthermore, no conditions are supplied at $\bar{t} = 0$, since transient effects are not to be investigated.

A solution to the system of Eqs. 4, with Eq. A2 replacing Eqs. 4d and 4e, is accomplished by utilizing the following superposition:

$$\bar{V}_{x_1} = \bar{V}_{x_p}(\bar{y}, \bar{t}) + \tilde{V}_{x_1}(\bar{x}, \bar{y}, \bar{t}) \tag{A3a}$$

$$\bar{V}_{y_1} = \bar{V}_{y_p}(\bar{t}) + \tilde{V}_{y_1}(\bar{x}, \bar{y}, \bar{t}) \tag{A3b}$$

$$\bar{P}_1 = \bar{P}_p(\bar{y}, \bar{t}) + \tilde{P}_1(\bar{x}, \bar{y}, \bar{t}) \tag{A3c}$$

$$\bar{\eta}_1 = \bar{\eta}_p(\bar{t}) + \tilde{\eta}_1(\bar{x}, \bar{t}) \tag{A3d}$$

In Eq. A3, the subscript p denotes the particular solution which satisfies the nonhomogeneous parts of conditions (Eqs. A2). Equations A3 are substituted into Eqs. 4 and A2, and the following boundary-value problem to obtain the particular solution is obtained:

$$Re\left(\frac{\partial\bar{V}_{x_p}}{\partial\bar{t}} + \bar{V}_{y_p}\frac{\partial\bar{V}_{x_0}}{\partial\bar{y}}\right) = \frac{\partial^2\bar{V}_{x_p}}{\partial\bar{y}^2} \tag{A4a}$$

$$Re\frac{d\bar{V}_{y_p}}{d\bar{t}} = -\frac{\partial\bar{P}_p}{\partial\bar{y}} \tag{A4b}$$

$$\begin{pmatrix} \bar{V}_{y_p} = \omega e^{-i\omega\bar{t}} \\ \bar{V}_{x_p} = -i\dfrac{d\bar{V}_{x_0}}{d\bar{y}} e^{-i\omega\bar{t}} \end{pmatrix} \quad \text{at} \quad \bar{y} = 1 \tag{A4c,d}$$

$$\begin{pmatrix} \bar{V}_{y_p} = \dfrac{d\bar{\eta}_p}{d\bar{t}} \\ \bar{P}_p + \dfrac{3\cot\gamma}{Re}\bar{\eta}_p = 0 \\ \dfrac{\partial\bar{V}_{x_p}}{\partial\bar{y}} = -\dfrac{d^2\bar{V}_{x_0}}{d\bar{y}^2}\bar{\eta}_p \end{pmatrix} \quad \text{at} \quad \bar{y} = 0 \tag{A4e,f,g}$$

Employing the result for $\bar{V}_{x_0}$ given by Eqs. 2a, the solution to the above system is given by:

$$\bar{V}_{x_p} = 3i\bar{y}e^{-i\omega\bar{t}} \tag{A5a}$$

$$\bar{V}_{y_p} = \omega e^{-i\omega\bar{t}} \tag{A5b}$$

$$\bar{P}_p = ie^{-i\omega\bar{t}}\left(\omega^2 Re\,\bar{y} - \frac{3\cot\gamma}{Re}\right) \tag{A5c}$$

$$\bar{\eta}_p = ie^{-i\omega\bar{t}} \tag{A5d}$$

The physical meaning of the particular solution results (Eqs. A5) is now given. By comparing the mathematical form of the wall oscillations given by Eq. A1 with Eq. A5d, it is clear that the particular solution describes an interface which is simply translating up and down as the wall oscillates, with no interfacial motion relative to the plate surface. This is further supported by Eq. A5b, which gives a perpendicular velocity consistent with this motion. The meaning of the result (Eq. A5a) is determined as follows. Using Eqs. 2a, A2a, A3a, and A5a, and ignoring the tilde contribution to the velocity for simplicity, the velocity $\overline{V}_x$ is given to $O(\epsilon)$ as:

$$\overline{V}_x \sim \frac{3}{2}(1-\bar{y}^2) + 3i\epsilon\bar{y}e^{-i\omega\bar{t}} \quad \text{as} \quad \epsilon \to 0 \tag{A6a}$$

This result is the asymptotic expansion of the following function [to $O(\epsilon)$] for small ϵ:

$$\overline{V}_x = \frac{3}{2}[1-(\bar{y}-i\epsilon e^{-i\omega\bar{t}})^2] \tag{A6b}$$

Using Eq. A1, Eq. A6b describes a uniform flow solution which is being displaced in the $\bar{y}$ direction with no perpendicular motion relative to the wall as the wall oscillates.

The remaining boundary-value problem for those variables denoted with a tilde ($\sim$) in Eq. A3 is identical to the system of Eqs. 4, where the tilde replaces the overbar on the dependent variables and the condition 4e is replaced with:

$$\tilde{V}_{x_1} = 0 \quad \text{at} \quad \bar{y} = 1 \tag{A7}$$

The system of Eqs. 4, using condition A7, is exactly the tilde system presented for the case of oscillations in the direction of flow, presented in the Theory section. Then, using the results given by Eqs. 9-13 as well as Eq. A5, the interface and velocity solutions are:

$$\overline{\eta}_{1_u} = ie^{-i\omega\bar{t}} + \sum_\theta A_\theta \frac{\alpha(\theta)\tilde{\psi}(0;\theta)}{[\theta - \alpha(\theta)\overline{V}_{x_0}(0)]} e^{i[\alpha(\theta)\bar{x} - \theta\bar{t}]} \tag{A8a}$$

$$\overline{V}_{x_{1_u}} = 3i\bar{y}e^{-i\omega\bar{t}} + \sum_\theta A_\theta \frac{d\tilde{\psi}}{d\bar{y}} e^{i[\alpha(\theta)\bar{x} - \theta\bar{t}]} \tag{A8b}$$

$$\overline{V}_{y_{1_u}} = \omega e^{-i\omega\bar{t}} - \sum_\theta i\alpha(\theta)A_\theta\tilde{\psi}(\bar{y};\theta)e^{i[\alpha(\theta)\bar{x} - \theta\bar{t}]} \tag{A8c}$$

where subscript u has been added to denote that Eqs. A8 are valid only in the uniform film region. In Eqs. A8, constants A_θ are undetermined since only the behavior in the uniform film region has been considered. The values for these constants are determined by considering the physics of the entrance region, which must match with the limiting forms given by Eqs. A8.

At this point, we note that the particular parts of the solution, that is, those terms not in the summations of Eqs. A8, contain all the effects due to the oscillating wall. On the other hand, the summation terms in each case, the solutions to the tilde system, are merely superpositions of traveling waves which do not interact with the oscillating wall. That is precisely the structure of the solution for the case where the wall was oscillating in the direction of flow. As is demonstrated by the experimental results presented in this article, the conditions at the entrance to the incline will determine the wavelength and eventual amplitude of the wave which is seen down the incline.

Manuscript received July 15, 1992, and revision received Jan. 11, 1993.